arXiv:1109.4188v1 [physics.acc-ph] 19 Sep 2011

Optical transition radiation in presence of acoustic waves for an oblique incidence

A. R. Mkrtchyan, V. V. Parazian*, A. A. Saharian†

Institute of Applied Problems in Physics,
25 Nersessian Street, 0014 Yerevan, Armenia

Abstract

Forward transition radiation is considered in an ultrasonic superlattice excited in a finite thickness plate under oblique incidence of relativistic electrons. We investigate the influence of acoustic waves on both the intensity and polarization of the radiation. In the quasi-classical approximation, formulas are derived for the vector potential of the electromagnetic field and for the spectral-angular distribution of the radiation intensity. It is shown that the acoustic waves generate new resonance peaks in the spectral and angular distributions. The heights and the location of the peaks can be controlled by choosing the parameters of the acoustic wave. The numerical examples are given for a plate of fused quartz.

Keywords: Interaction of particles with matter; physical effects of ultrasonics.

PACS Nos.: 41.60.Dk, 43.35.Sx, 43.35.-c

1 Introduction

Transition radiation is produced when a uniformly moving charged particle crosses an interface between two media with different dielectric properties. Such radiation has a number of remarkable properties and at present it has found many important applications (see, for instance, Refs. [1]-[6]). In particular, the transition radiation is widely used for particle identification, for the measurement of transverse size, divergence and energy of electron and proton beams. An enhancement for the transition radiation intensity may be achieved by using the interference between the radiation emitted by many interfaces in a multilayer structure. From the point of view of controlling the parameters of various radiation processes in a medium, it is of interest to investigate the influence of external fields, such as acoustic waves, temperature gradient etc., on the corresponding characteristics. The considerations of processes, such as diffraction radiation [7], parametric X-radiation [8], channeling radiation [9], bremsstrahlung of high-energy electrons [10], electron-positron pair creation by high-energy photons [11], have shown that the external fields can remarkably change the spectral and angular characteristics of the radiation intensities. Recently there has been broad interest in compact crystalline undulators with periodically deformed crystallographic planes as an efficient source of high energy photons (for a review see Ref. [12]).

*E mail: vparazian@gmail.com
†E mail: saharian@ysu.am

In Refs. [13, 14] we have considered the X-ray and optical transition radiation from ultra-relativisitic electrons in an ultrasonic superlattice excited in melted quartz plate. The radiation from a charged particle for a semi-infinite laminated medium has been recently discussed in [15]. In these references the transition radiation is considered under normal incidence of a charged particle upon the interface of the plate. In the present paper we generalize the corresponding results for oblique incidence. The angle between the particle velocity and the normal to the interface is an additional parameter which can be used for the control of angular-frequency distribution and the polarization of the radiation.

We have organized the paper as follows. In the next section we evaluate the vector potential for the electromagnetic field by using the quasi-classical approximation. The intensity of the radiation in forward direction is investigated in section 3 for both parallel and perpendicular polarizations. In section 4 we present numerical examples for the radiation intensity in the case of a plate made of fused quartz. The main results of the paper are summarized in section 5.

2 Electromagnetic field

We consider the transition radiation under oblique incidence of a charged particle on a plate with dielectric permittivity ε_0 which is immersed into a homogeneous medium with permittivity ε_1. We assume that the plate has the thickness l and its boundaries are located at $z=-l$ and $z=0$. In what follows the z axis is directed along the normal to the plate. The trajectory of the particle with velocity $\mathbf{v}$ is in the (x,z) plane and forms with the z axis a given angle α. So, we can write $\mathbf{v}=(v\sin\alpha,0,v\cos\alpha)$. We assume that longitudinal ultrasonic vibrations are excited in the plate along the normal to its surface, that form a superlattice. In the presence of the ultrasonic waves, the dielectric permittivity can be written in the form

$$\varepsilon(z)=\begin{cases}\varepsilon_0+\Delta\varepsilon\cos\left(k_s z+\omega_s t+\phi\right), & -l\leqslant z\leqslant 0,\\ \varepsilon_1, & z<-l,\ z>0,\end{cases}. \tag{1}$$

In (1), ω_s, k_s are the cyclic frequency and the wave number of the ultrasound, and ϕ is the initial phase. Under the condition $\nu_s l/v\ll 1$, with $\nu_s=\omega_s/(2\pi)$, during the transit time of the particle the dielectric permittivity in the superlattice is not notably changed. For relativistic particles and for the plate thickness $l\lesssim 1$ cm this leads to the constraint $\nu_s\ll 10^{11}$ Hz.

Here we are interested in the radiation with frequencies ω in the spectral range $\omega\gg k_s c$. The presence of the small parameter $k_s c/\omega$ allows us to employ the quasi-classical approximation for the evaluation of the radiation field in the forward direction. It is natural that in this case the plate boundaries must be sufficiently smooth. This condition is assumed to be observed [1] because the transition radiation on these boundaries is formed in a zone with macroscopic length. For the current density one has the expression

$$\mathbf{j}=e\mathbf{v}\delta\left(x-x\left(t\right)\right)\delta\left(y\right)\delta\left(z-z\left(t\right)\right), \tag{2}$$

where e is the charge of the particle and

$$x\left(t\right)=v\left(t-t_0\right)\sin\alpha,\ z\left(t\right)=-l+v\left(t-t_0\right)\cos\alpha. \tag{3}$$

Here we assume that the particle trajectory is rectilinear (for the discussion of multiple scattering effects see [1]).

In the Lorentz gauge, the vector potential of the electromagnetic field corresponding to the source (2) can be taken as $\mathbf{A}=(A_x,0,A_z)$. We define the partial Fourier transform as

$$\mathbf{A}\left(\omega,\mathbf{q},z\right)=\frac{1}{(2\pi)^3}\int dt\int d\mathbf{r}_\perp\,\mathbf{A}\left(t,\mathbf{r}\right)e^{i(\omega t-\mathbf{q}\mathbf{r}_\perp)}, \tag{4}$$

with $\mathbf{q}=(k_x,k_y)$ and $\mathbf{r}_\perp=(x,y)$. In the quasi-classical approximation, these components are determined by the following expressions [16] (see also [1] for the discussion of applicability of this approximation)

$$\begin{aligned} A_x(\omega,\mathbf{q},z) &= \frac{-i}{2k_z^{1/2}(z)}\int dz' \frac{F_x(z')}{k_z^{1/2}(z')}\exp\left(i\int_{z'}^{z} dz'' k_z(z'')\right), \\ A_z(\omega,\mathbf{q},z) &= -\frac{i\sqrt{\varepsilon(z)}}{2k_z^{1/2}(z)}\int dz' \frac{\sqrt{\varepsilon(z')}}{k_z^{1/2}(z')}\exp\left(i\int_{z'}^{z} dz'' k_z(z'')\right) \\ &\quad\times\left[\frac{F_z(z')}{\varepsilon(z')}+\frac{ik_x}{\varepsilon^2(z')}\frac{d\varepsilon(z')}{dz'}A_x(\omega,\mathbf{q},z')\right]. \end{aligned} \tag{5}$$

In (5), we have defined the functions

$$k_z(z)=\sqrt{\frac{\omega^2}{c^2}\varepsilon(z)-q^2}, \tag{6}$$

and

$$F_p(z)=-\frac{1}{2\pi^2 c}\int dt\int d\mathbf{r}_\perp\; j_p(\mathbf{r},t)\,e^{i(\omega t-\mathbf{q}\mathbf{r}_\perp)}, \tag{7}$$

with $p=x,z$.

For the problem under consideration, by using the expressions for the components of the current density, the functions $F_p(z)$ are written in the form

$$\begin{aligned} F_z(z) &= -\frac{ee^{i\omega t_0}}{2\pi^2 c}\exp\left[i\frac{z+l}{v\cos\alpha}(\omega-k_x v\sin\alpha)\right], \\ F_x(z) &= F_z(z)\tan\alpha \end{aligned} \tag{8}$$

Assuming that $\Delta\varepsilon$ is sufficiently small, which is well satisfied for the perturbations induced by the ultrasound, for the function (6) we can write

$$k_z(z)=\begin{cases} k_z^{(1)}, & z<-l,\ z>0, \\ k_z^{(0)}+ak_s\cos(k_s z+\varphi_1), & -l\leqslant z\leqslant 0, \end{cases} \tag{9}$$

with $\varphi_1=\omega_s t_0+\phi$. Here and in what follows we use the notations

$$k_z^{(j)} = \sqrt{\omega^2\varepsilon_j/c^2-q^2},\ j=0,1, \tag{10}$$

$$a = \frac{\omega^2\Delta\varepsilon}{2c^2k_s k_3^{(0)}}. \tag{11}$$

Note that $a\sim\lambda_s\Delta\varepsilon/\lambda$, where λ_s is the wavelength of the acoustic wave and λ is the wavelength for the radiated photon.

Substituting expressions (8) into (5) and using the relation

$$e^{ib\sin\tau}=\sum_{m=-\infty}^{+\infty}J_m(b)\,e^{im\tau}, \tag{12}$$

with $J_m(b)$ being the Bessel function of the first kind, after the integration, for the components of the vector potential in the region $z>0$ one finds

$$\begin{aligned} A_x(\omega,\mathbf{q},z) &= \frac{ee^{i\omega t_0+ik_z^{(1)}z}}{4\pi^2 ck_z^{(1)}}\tan\alpha\left[C_1(\omega,\mathbf{q})+2iC_2(\omega,\mathbf{q})\right], \\ A_z(\omega,\mathbf{q},z) &= \frac{ee^{i\omega t_0+ik_z^{(1)}z}}{4\pi^2 ck_z^{(1)}}\left[C_1(\omega,\mathbf{q})+2i\sqrt{\varepsilon_1/\varepsilon_0}C_2(\omega,\mathbf{q})\right]. \end{aligned} \tag{13}$$

In these expressions we have defined the functions

$$
\begin{aligned}
C_1(\omega,\mathbf{q}) &= \frac{e^{ik_z^{(0)}l+ia[\sin(k_sl-\varphi_1)+\sin(\varphi_1)]}-e^{il(\omega/v_z-k_x\tan\alpha)}}{\omega/v_z-k_x\tan\alpha-k_z^{(1)}},\\
C_2(\omega,\mathbf{q}) &= \sqrt{\frac{k_z^{(1)}}{k_z^{(0)}}}e^{ia\sin\varphi_1}\sum_{m=-\infty}^{+\infty}J_m(a)e^{ilk_{zm}^{(0)}/2-im\varphi_1}\\
&\quad\times\frac{\sin[(\omega/v_z-k_x\tan\alpha-k_{zm}^{(0)})l/2]}{\omega/v_z-k_x\tan\alpha-k_{zm}^{(0)}},
\end{aligned}
\tag{14}
$$

with $v_z=v\cos\alpha$ and

$$
k_{zm}^{(0)}=k_z^{(0)}+mk_s. \tag{15}
$$

For a special case $\alpha=0$ we have $A_x(\omega,\mathbf{q},z)=0$ and the expression for $A_z(\omega,\mathbf{q},z)$ coincides with the formula previously obtained in [14] for the normal incidence.

3 Radiation intensity

Given the vector potential we can evaluate the radiation intensity in the region $z>0$. First we consider the total radiation intensity. The energy flux through the plane $z=$const is given by the integration of the z-projection of the Poynting vector:

$$
\frac{c}{4\pi}\int dxdydt[\mathbf{EH}]_z=4\pi^2c\int d\omega\int d\mathbf{q}\,[\mathbf{E}(\omega,\mathbf{q},z)\mathbf{H}^*(\omega,\mathbf{q},z)]_z, \tag{16}
$$

where for the Fourier components of the electric and magnetic fields we have the expressions

$$
\mathbf{H}(\omega,\mathbf{q},z)=i[\mathbf{k}\,\mathbf{A}(\omega,\mathbf{q},z)],\ \mathbf{E}(\omega,\mathbf{q},z)=-\frac{c}{\omega\varepsilon_1}[\mathbf{k}\,\mathbf{H}(\omega,\mathbf{q},z)], \tag{17}
$$

with $\mathbf{k}=(k_x,k_y,k_z^{(1)})$. By using these relations for the spectral-angular density of the radiation intensity we find

$$
I(\omega,\theta,\varphi)=\frac{d\mathcal{I}(\omega,\theta,\varphi)}{d\omega d\theta d\varphi}=4\pi^2\sqrt{\varepsilon_1}\frac{\omega^2}{c}\sin\theta\cos^2\theta\,|[\mathbf{k}\,\mathbf{A}(\omega,\mathbf{q},z)]|^2, \tag{18}
$$

where θ and φ are the polar and azimuthal angles for the radiated photon wave vector:

$$
\mathbf{k}=\frac{\omega}{c}\sqrt{\varepsilon_1}(\sin\theta\cos\varphi,\sin\theta\sin\varphi,\cos\theta). \tag{19}
$$

By taking into account the expressions (13) and (14) for the components of the vector potential, after the averaging over the phase φ_1 of particle flight into the plate, for the spectral-angular density of the radiated energy in the angular region with $\sin\theta<\sqrt{\varepsilon_0/\varepsilon_1}$ we find the expression

$$
\begin{aligned}
I(\omega,\theta,\varphi) &= \frac{e^2\sin^3\theta\cos^2\alpha}{\pi^2c\sqrt{\varepsilon_1}}\sum_{m=-\infty}^{+\infty}J_m^2\left(\frac{\omega\Delta\varepsilon/(2ck_s)}{\sqrt{\varepsilon_0-\varepsilon_1\sin^2\theta}}\right)\\
&\quad\times\left[\frac{\mathbf{P}(\theta,\varphi,\alpha)}{V(\theta,\varphi,\alpha)}-\frac{\mathbf{Q}(\theta,\varphi,\alpha)}{U_m(\theta,\varphi,\alpha)}\frac{\cos^{1/2}\theta}{(\varepsilon_0/\varepsilon_1-\sin^2\theta)^{1/4}}\right]^2\\
&\quad\times\sin^2\left[\frac{\omega l\sqrt{\varepsilon_1}}{2c\cos\alpha}U_m(\theta,\varphi,\alpha)\right].
\end{aligned}
\tag{20}
$$

In (20) we have defined the functions

$$\begin{aligned} U_m(\theta,\varphi,\alpha) &= 1/\beta_1 - \sin\theta\cos\varphi\sin\alpha - \cos\alpha\sqrt{\varepsilon_0/\varepsilon_1 - \sin^2\theta} - \frac{mk_sc}{\omega\sqrt{\varepsilon_1}}\cos\alpha, \\ V(\theta,\varphi,\alpha) &= 1/\beta_1 - \sin\theta\cos\varphi\sin\alpha - \cos\theta\cos\alpha, \end{aligned} \tag{21}$$

and the vectors

$$\begin{aligned} \mathbf{P}(\theta,\varphi,\alpha) &= (\sin\varphi, \cot\theta\tan\alpha - \cos\varphi, -\sin\varphi\tan\alpha), \\ \mathbf{Q}(\theta,\varphi,\alpha) &= (\sqrt{\varepsilon_1/\varepsilon_0}\sin\varphi, \cot\theta\tan\alpha - \sqrt{\varepsilon_1/\varepsilon_0}\cos\varphi, -\sin\varphi\tan\alpha), \end{aligned} \tag{22}$$

with $\beta_1 = v\sqrt{\varepsilon_1}/c$. In general, ε_0 and ε_1 are functions of ω. In the case of normal incidence the general formula (20) coincides with the result previously derived in [14]. In the discussion below we will assume that $\beta_1 < 1$.

Unlike to the case of the normal incidence, in the problem under consideration we have two different polarizations. For the first one the electric field for the radiation is parallel to the observation plane (plane formed by the vectors $\mathbf{k}$ and $\mathbf{v}$) and for the second one the electric field is perpendicular to the observation plane. These two polarizations are referred as parallel and perpendicular polarizations, respectively. The spectral-angular densities for these polarizations we will denote by $I_{\parallel}(\omega,\theta,\varphi)$ and $I_{\perp}(\omega,\theta,\varphi)$. The radiation intensity for the perpendicular polarization is determined by the z-projection of the corresponding integrated Poynting vector which is given by expression (16) with the replacement $\mathbf{E}(\omega,\mathbf{q},z) \to \mathbf{E}_{\perp}(\omega,\mathbf{q},z)$, where $\mathbf{E}_{\perp}(\omega,\mathbf{q},z)$ is the component of the electric field perpendicular to the observation plane. Now, by taking into account that

$$[\mathbf{E}_{\perp}(\omega,\mathbf{q},z)\mathbf{H}^*(\omega,\mathbf{q},z)]_z = \frac{\omega^2}{c^2}\sqrt{\varepsilon_1}\cos\theta|\mathbf{A}_{\perp}(\omega,\mathbf{q},z)|^2, \tag{23}$$

for the spectral-angular density of the corresponding radiation intensity one finds

$$I_{\perp}(\omega,\theta,\varphi) = 4\pi^2\frac{\omega^4}{c^3}\varepsilon_1^{3/2}\sin\theta\cos^2\theta|\mathbf{A}_{\perp}(\omega,\mathbf{q},z)|^2. \tag{24}$$

By making use of expressions (13) and (14), after averaging over the phase φ_1, we get the following final expression

$$\begin{aligned} I_{\perp}(\omega,\theta,\varphi) &= \frac{e^2}{4\pi^2 c}\frac{\left(1-\sqrt{\varepsilon_1/\varepsilon_0}\right)^2}{\sqrt{\varepsilon_0 - \varepsilon_1\sin^2\theta}}\sin^3\theta\cos\theta\sin^2\varphi\sin^2(2\alpha) \\ &\times \sum_{m=-\infty}^{+\infty} J_m^2\left(\frac{\omega\Delta\varepsilon/(2ck_s)}{\sqrt{\varepsilon_0 - \varepsilon_1\sin^2\theta}}\right) U_m^{-2}(\theta,\varphi) \\ &\times \sin^2\left[\frac{\omega l\sqrt{\varepsilon_1}}{2c\cos\alpha}U_m(\theta,\varphi)\right]. \end{aligned} \tag{25}$$

As we have already noted, the radiation intensity for the perpendicular polarization vanishes in the case of the normal incidence and this is explicitly seen from (25). The radiation intensity for the parallel polarization is found from the relation

$$I_{\parallel}(\omega,\theta,\varphi) = I(\omega,\theta,\varphi) - I_{\perp}(\omega,\theta,\varphi) \tag{26}$$

with the total intensity given by (20).

The radiation intensities for both polarizations have peaks corresponding to the zeros of the function $U_m(\theta,\varphi,\alpha)$. The angular location of the peaks is determined from the equation

$$\sin\theta\cos\varphi\sin\alpha + \cos\alpha\sqrt{\varepsilon_0/\varepsilon_1 - \sin^2\theta} = 1/\beta_1 - \frac{mk_sc}{\omega\sqrt{\varepsilon_1}}\cos\alpha. \tag{27}$$

Note that the location of the peaks does not depend on the amplitude of the acoustic oscillations (within the framework of the approximation used). The amplitude will determine the heights of the peaks. The last term in the right-hand side of (27) is induced by the acoustic waves. This term is of the order $(\omega_s/\omega)(c/v_s)$, with v_s being the velocity for the acoustic waves. In the presence of acoustic waves we have a set of peaks specified by m. The angular location of the peak with $m = 0$ coincides with that for the peak in the absence of acoustic waves. The angular distance between the peaks induced by the acoustic waves is of the order $(\omega_s/\omega)(c/v_s)$. The condition (27) can be written in a physically more transparent form if, in addition to (19), we introduce the wave vector $\mathbf{k}_0$ for the photon inside the plate (in the absence of the acoustic wave), with the components

$$\mathbf{k}_0 = \frac{\omega}{c}\sqrt{\varepsilon_0}\,(\sin\theta_0\cos\varphi, \sin\theta_0\sin\varphi, \cos\theta_0)\,, \tag{28}$$

where $\sin\theta_0 = \sqrt{\varepsilon_1/\varepsilon_0}\sin\theta$ (note that the azimuthal angle φ is the same inside and outside the plate). Now it can be seen that, with the help of this vector, the condition for the peaks is written in the form

$$\mathbf{k}_{0m}\mathbf{v} = \omega,\ \mathbf{k}_{0m} \equiv \mathbf{k}_0 + m\mathbf{k}_s, \tag{29}$$

with $\mathbf{k}_s = (0, 0, k_s)$. The latter is the Cherenkov condition for the medium of the plate. Hence, we conclude that the peaks in the region $z > 0$, determined by the condition (27), correspond to the Cherenkov radiation emitted inside the plate and refracted from the boundary. We can have a situation where the Cherenkov radiation emitted inside the plate is completely reflected from the boundary and in the exterior region we have no peaks. In this case the equation (27) has no solutions. We can also have cases then the Cherenkov radiation is confined inside the plate in the absence of the acoustic excitations and the peaks defined by (27) appear as a result of the influence of the acoustic waves. Note that the location of the peaks can also be controlled by choosing the incidence angle α.

Various special cases of formulas (20) and (25) can be considered. In the case of the normal incidence the radiation intensity for the perpendicular polarization vanishes and for the parallel polarization we recover the results of Refs. [13] and [14] for the X-ray and optical transition radiations respectively. In the absence of the acoustic wave we have $\Delta\varepsilon = 0$ and in formulas (20) and (25) the $m = 0$ term contributes only. In this case we obtain the quasi-classical approximation for the radiation intensity for oblique incidence. The corresponding exact expression for the radiation intensity in this problem is well known from the literature [17] (see also Refs. [1]-[6]). The features of the optical transition radiation in a finite thickness plate for an oblique incidence have been discussed in Refs. [18] on the base of Pafomov's formulas. For a transparent material in the over-threshold case and under the condition $l\omega/v \gg 1$, the dominant contribution comes from the term in the exact formula with the resonant factor $\sin^2(y)/y^2$, with y given by the argument of the sin function in (20) with $m = 0$. Now, for simplicity considering the case of the radiation into the vacuum, it can be seen that for a relativistic particle with $1 - v/c \ll 1$, the radiation intensity near the Cherenkov peaks is well approximated by the formulas obtained from (20) and (25) in the limit $\Delta\varepsilon = 0$.

For given values of α and φ, the equation (27) determines the location of the peaks with respect to the polar angle θ. We will denote the corresponding values by $\theta^{(m)}$. At the peaks the total radiation intensity is given by the expressions

$$I(\omega, \theta^{(m)}, \varphi) = \frac{e^2\varepsilon_1 l^2\omega^2 \sin^3\theta^{(m)}\cos\theta^{(m)}}{4\pi^2 c^3(\varepsilon_0 - \varepsilon_1\sin^2\theta^{(m)})^{1/2}}$$
$$\times \mathbf{Q}^2(\theta^{(m)}, \varphi, \alpha) J_m^2\left(\frac{\omega\Delta\varepsilon/(2ck_s)}{\sqrt{\varepsilon_0 - \varepsilon_1\sin^2\theta^{(m)}}}\right). \tag{30}$$

For the relative contribution of the component with the perpendicular polarization one gets

$$\frac{I_{\perp}\left(\omega,\theta^{(m)},\varphi\right)}{I\left(\omega,\theta^{(m)},\varphi\right)}=\left(1-\sqrt{\varepsilon_1/\varepsilon_0}\right)^2\frac{\sin^2\varphi\sin^2\alpha}{\mathbf{Q}^2(\theta^{(m)},\varphi,\alpha)}. \tag{31}$$

In the absence of the ultrasonic vibrations the location of the peak is given by $\theta^{(0)}$. The ultrasound reduces the height of this peak by the factor $J_0^2\left(\omega\Delta\varepsilon/(2ck_s\sqrt{\varepsilon_0-\varepsilon_1\sin^2\theta^{(0)}})\right)$. In particular, for a given radiation frequency, the frequency or the amplitude of the ultrasound can be tuned to eliminate this peak (see the numerical example below).

In the limit $l\to\infty$, by using the formula $\lim_{x\to\infty}\sin^2(ux)/x=\pi u^2\delta(u)$, with $\delta(u)$ being the Dirac delta function, for the spectral-angular density of the total radiation energy per unit length we find

$$\begin{aligned}I_{\infty}\left(\omega,\theta,\varphi\right)=&\frac{e^2\omega\sin^3\theta\cos\theta\cos\alpha}{2\pi c^2\sqrt{\varepsilon_0/\varepsilon_1-\sin^2\theta}}\delta\left[U_m(\theta,\varphi,\alpha)\right]\\&\times\mathbf{Q}^2(\theta,\varphi,\alpha)\sum_{m=-\infty}^{+\infty}J_m^2\left(\frac{\omega\Delta\varepsilon/(2ck_s)}{\sqrt{\varepsilon_0-\varepsilon_1\sin^2\theta}}\right),\end{aligned} \tag{32}$$

where $I_{\infty}\left(\omega,\theta,\varphi\right)=\lim_{l\to\infty}I\left(\omega,\theta,\varphi\right)/l$. A similar formula is obtained from (25) for the perpendicular polarization. In this case the radiation along a given direction has discrete spectrum $\omega=\omega_m$, determined by the relation $U_m(\theta,\varphi,\alpha)=0$, or explicitly

$$\omega_m=\frac{|m|k_sv\cos\alpha}{|1-\beta_1\sin\theta\cos\varphi\sin\alpha-\beta_1\cos\alpha\sqrt{\varepsilon_0/\varepsilon_1-\sin^2\theta}|}. \tag{33}$$

The spectral distribution of the radiation intensity is obtained from (32) by the integration over θ and φ.

4 Radiation in a plate of fused quartz

Having the general analysis for the radiation intensity, we turn to numerical examples. We will be interested in the optical transition radiation. For the numerical evaluation of the radiation intensity the material of the plate should be specified. We assume that the plate is made of fused quartz with the velocity of longitudinal ultrasonic vibrations $v_s\approx 5.6\times10^5$ cm/s. For the corresponding dielectric permittivity we use the Sellmeier dispersion formula

$$\varepsilon_0=1+\sum_{i=1}^{3}\frac{a_i\lambda^2}{\lambda^2-l_i^2} \tag{34}$$

with the parameters $a_1=0.6961663$, $a_2=0.4079426$, $a_3=0.8974794$, $l_1=0.0684043$, $l_2=0.1162414$, $l_3=9.896161$. In (34), λ is the wavelength of the radiation measured in micrometers. Formula (34) well describes the dispersion properties of fused quartz in the range $0.2\mu\text{m}\leqslant\lambda\leqslant 6.7\mu\text{m}$. In this spectral range fused quartz is very weakly absorbing.

In figures below we plot the spectral-angular density of the total radiation intensity in the forward direction, $I(\omega,\theta,\varphi)/\hbar$, and the spectral-angular density for the component with perpendicular polarization, $I_{\perp}(\omega,\theta,\varphi)/\hbar$, for electrons with the energy 2 MeV and for the plate thickness $l=1$ cm. For the oscillation amplitude we have taken the value $\Delta n/n_0=0.05$, where n_0 is the number of electrons per unit volume for fused quartz.

As it is seen from the graphs and in accordance with general features described above, the presence of the acoustic wave leads to the appearance of new peaks in both angular and spectral distributions of the radiation intensity. The height of the peaks can be tuned by choosing the parameters of the acoustic wave. In particular, the peak in the radiation intensity which is present in the absence of the acoustic wave is reduced by the factor $J_0^2(a)$, where a is the argument of the Bessel function in (20). In particular, this peak can be completely removed by taking the parameters of the acoustic wave in such a way to have $a = j_{0,s}$, $s = 1, 2, 3, \ldots$, where $z = j_{0,s}$ are the zeroes of the function $J_0(z)$.

In figure 1 we plot the radiation intensity, defined by (20), as a function of the polar angle θ for separate values of the angle α (numbers near the curves) and for the cyclic frequency $\omega = 2.73 \times 10^{14}$ Hz. For the azimuthal angle we have taken the value $\varphi = 0.369$. The graphs in figure 1 are plotted for the frequency of acoustic wave $\nu_s = 5$ MHz. Dashed curves correspond to the radiation in the situation where the acoustic wave is absent. Left and right panels show two different sets of the peaks. Similar graphs for the radiation with the perpendicular polarization are displayed in figure 2 for the same values of the parameters. The peaks in the spectral distribution of the radiation intensity for a polar angle $\theta = 0.253$ are shown in figure 3 for the total intensity (left panel) and for the radiation with perpendicular polarization (right panel). The values of the other parameters are the same as those for figure 1. In figure 4 we show the spectral distribution for the total intensity (left panel) and for the intensity of the radiation with perpendicular polarization (right panel) for separate values of the acoustic wave frequency ν_s (numbers near the curves). An example is presented where the $m = 0$ peak in the absence of the acoustic wave is completely suppressed by the acoustic wave.

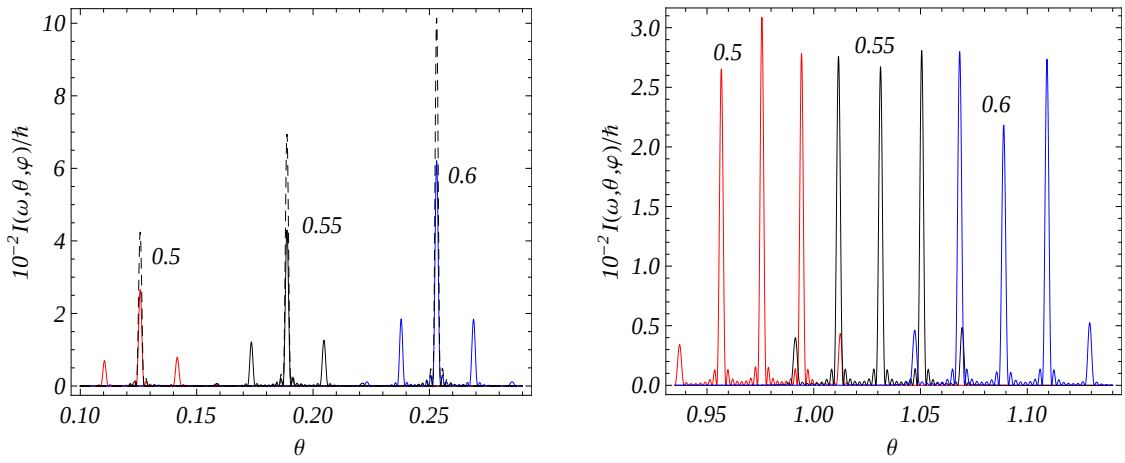


Figure 1: The angular distributions of the radiation intensity for two separate sets of peaks for different values of the incidence angle α (numbers near the curves). The dashed curves correspond to the transition radiation in the case where the acoustic wave is absent. The values of the parameters are as follows: $\omega = 2.73 \times 10^{14}$ Hz, $\varphi = 0.369$, $\nu_s = 5$ MHz.

5 Conclusion

We have investigated the transition radiation under oblique incidence of a charged particle in the presence of acoustic waves. In the quasi-classical approximation, formulas are derived for vector potential of the electromagnetic field and for the radiation intensity in the forward direction. The spectral-angular density of the radiated energy is given by formula (20) for the total radiation

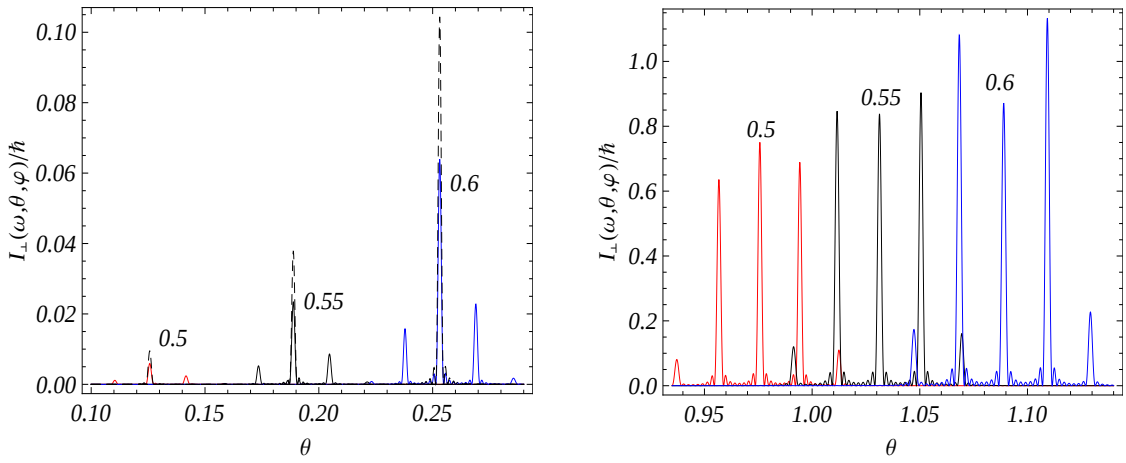


Figure 2: The same as in figure 1 for the perpendicular polarization.

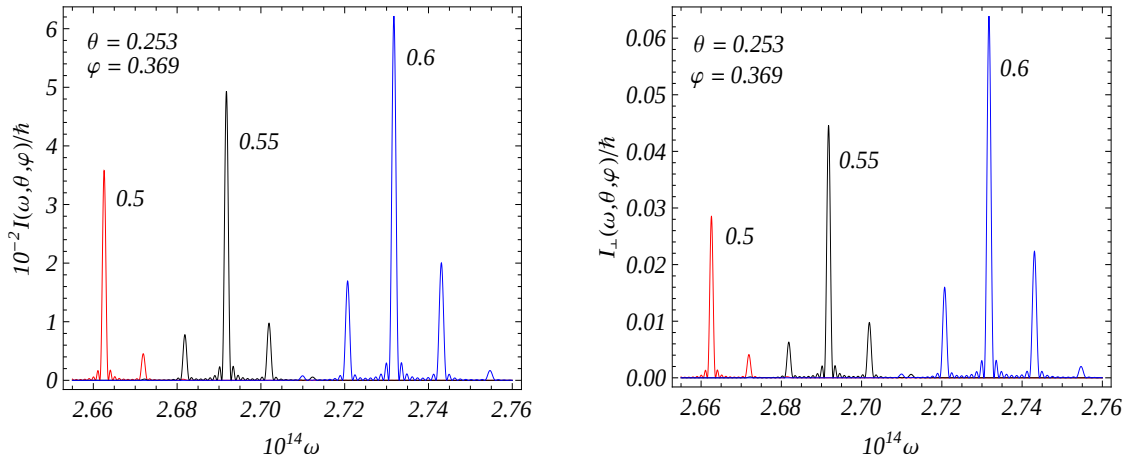


Figure 3: The spectral distribution of the radiation intensity for a polar angle $\theta = 0.253$ for the total intensity (left panel) and for the radiation with perpendicular polarization (right panel). The values of the other parameters are the same as those for figure 1.

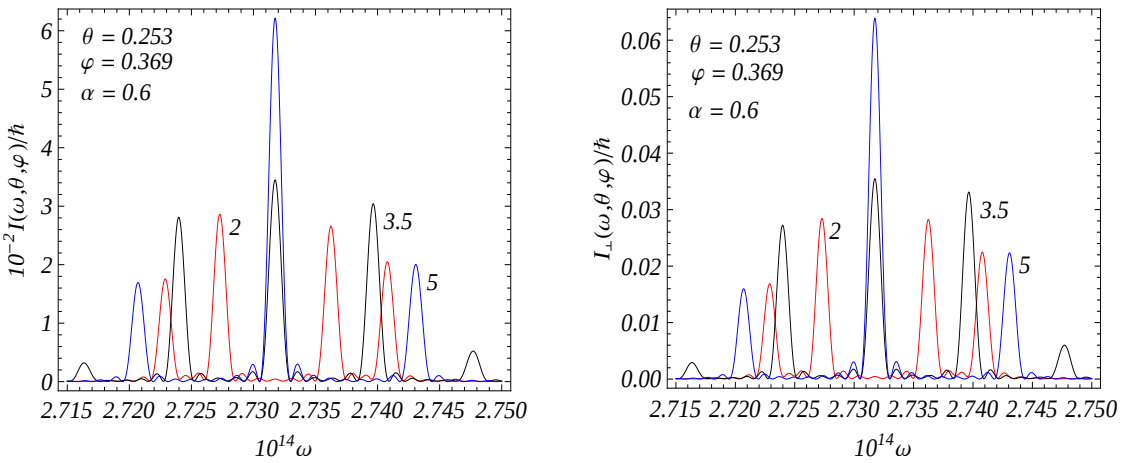


Figure 4: Spectral distribution for the total intensity (left panel) and for the intensity of the radiation with perpendicular polarization (right panel) for separate values of the acoustic wave frequency ν_s (numbers near the curves).

and by (25) for the component with perpendicular polarization. The radiation intensities for both polarizations have strong peaks with the angular location determined from the condition (27). This condition is written in a physically more transparent form, Eq. (29), in terms of the photon wave vector inside the plate. The latter clearly shows that the peaks correspond to the Cherenkov radiation emitted inside the plate and refracted from the boundary. In the presence of acoustic waves we have a set of peaks specified by m. The angular distance between them is of the order $(\omega_s/\omega)(c/v_s)$. The radiation intensity at the peaks is given by expressions (30) and (31). The angular-frequency parameters of the peaks can be controlled by tuning the amplitude and the wavelength of the ultrasound. In particular, we can have a situation where the peaks in the forward direction are absent in the absence of the acoustic excitations and they appear as a result of the influence of the acoustic waves. The numerical examples are given for the optical transition radiation in a plate of fused quartz. These results show that the acoustic waves allow to control the both angular and spectral parameters of the radiation. In particular, new resonance peaks appear in the spectral-angular distribution of the radiation intensity. An additional parameter which can be used for the control is the incidence angle.

6 Acknowledgment

The authors are grateful to Professors Babken Khachatryan and Levon Grigoryan for valuable discussions and suggestions.

References

[1] M. L. Ter-Mikaelian, *High Energy Electromagnetic Processes in Condensed Media* (Wiley Interscience, New York, 1972).

[2] G.M. Gharibian, S. Yan, *Rentgenovskoye Perekhodnoye Izluchenie* (Izd. AN Arm. SSR, Yerevan, 1983, in Russian).

[3] V. L. Ginzburg and V. N. Tsytovich, *Transition Radiation and Transition Scattering* (Adam Hilger, Bristol, 1990).

[4] V. N. Baier, V. M. Katkov, V. M. Strakhovenko, *Electromagnetic Processes at High Energies in Oriented Single Crystals* (World Scientific, Singapore, 1998).

[5] P. Rullhusen, X. Artru, P. Dhez, *Novel Radiation Sources Using Relativistic Electrons* (World Scientific, Singapore, 1998).

[6] A. P. Potylitsin, *Izluchenie Electronov v Periodicheskikh Structurakh* (Izdatelstvo Nauchno-Tekhnicheskoi Literaturi, Tomsk, 2009, in Russian).

[7] A. R. Mkrtchyan, L. Sh. Grigoryan, A. A. Saharian, A. N. Didenko, Acustica **75**, 1984 (1991); A. A. Saharian, A. R. Mkrtchyan, L. A. Gevorgian, L. Sh. Grigoryan, B. V. Khachatryan, Nucl. Instr. Meth. B **173**, 211 (2001).

[8] A. R. Mkrtchyan, H. A. Aslanyan, A. H. Mkrtchyan, R. A. Gasparyan, Phys. Lett. A **152**, 297 (1991).

[9] A. R. Mkrtchyan, R. A. Gasparyan, R. G. Gabrielyan, Phys. Lett. A **115**, 410 (1986); JETP **93** 432 (1987); Phys. Lett. A **126**, 528 (1988); L. Sh. Grigoryan et al., Nucl. Instr. Meth. B **173**, 132 (2001); **173**, 184 (2001); L. Sh. Grigoryan, A. H. Mkrtchyan, H. F. Khachatryan, V. U. Tonoyan, W. Wagner, Nucl. Instr. Meth. B **201**, 25 (2003); L. Sh. Grigoryan et al., Nucl. Instr. Meth. B **212**, 51 (2003).

[10] A. R. Mkrtchyan, A. A. Saharian, L. Sh. Grigoryan, B. V. Khachatryan, Mod. Phys. Lett. A **17**, 2571 (2002); A. R. Mkrtchyan, A. A. Saharian, V. V. Parazian, Mod. Phys. Lett. B **20**, 1617 (2006).

[11] A. A. Saharian, A. R. Mkrtchyan, V. V. Parazian, L. Sh. Grigoryan, Mod. Phys. Lett. A **19**, 99 (2004); A. R. Mkrtchyan, A. A. Saharian, V. V. Parazian, Mod. Phys. Lett. B **23**, 2573 (2009).

[12] A. V. Korol, A. V. Solov'yov and W. Greiner, Int. J. Mod. Phys. E **13**, 867 (2004).

[13] L. Sh. Grigoryan, A. H. Mkrtchyan, A. A. Saharian, Nucl. Instr. Meth. B **145**, 197 (1998).

[14] A. R. Mkrtchyan, V. V. Parazian, A. A. Saharian, Mod. Phys. Lett. B **24**, 2693 (2010).

[15] L. Sh. Grigoryan, A. R. Mkrtchyan, H. F. Khachatryan, S. R. Arzumanyan, W. Wagner, J. Phys.: Conference Series **236**, 012012 (2010); arXiv:0911.3494.

[16] B. V. Khachatryan, Doctor of Sciences Thesis. Yerevan, 2004 (in Russian).

[17] V. E. Pafomov, Proc. FIAN SSSR, Nuclear Physics and Particle Interaction with Matter, Vol. 44, Nauka, Moscow, 1969, p. 90.

[18] J. Ružička, J. Mehes, Nucl. Instr. Meth. A **250**, 491 (1986); A. Hrmo, J. Ruzicka, Nucl. Instrum. Methods A **451**, 506 (2000).